ACS APPLIED MATERIALS & INTERFACES

Letter

www.acsami.org

# Screen Printing of Highly Loaded Silver Inks on Plastic Substrates Using Silicon Stencils

Woo Jin Hyun,[†] Sooman Lim,[†] Bok Yeop Ahn,[‡] Jennifer A. Lewis,[‡] C. Daniel Frisbie,*[,†] and Lorraine F. Francis*[,†]

[†]Department of Chemical Engineering and Materials Science, University of Minnesota, 421 Washington Avenue SE, Minneapolis, Minnesota 55455, United States

[‡]School of Engineering and Applied Science, Wyss Institute for Biologically Inspired Engineering, Harvard University, 52 Oxford Street. Cambridge, Massachusetts 02138, United States

Supporting Information

**ABSTRACT:** Screen printing is a potential technique for mass-production of printed electronics; however, improvement in printing resolution is needed for high integration and performance. In this study, screen printing of highly loaded silver ink (77 wt %) on polyimide films is studied using fine-scale silicon stencils with openings ranging from 5 to 50 $\mu$m wide. This approach enables printing of high-resolution silver lines with widths as small as 22 $\mu$m. The printed silver lines on polyimide exhibit good electrical properties with a resistivity of $5.5 \times 10^{-6}$ $\Omega$ cm and excellent bending tolerance for bending radii greater than 5 mm (tensile strains less than 0.75%).

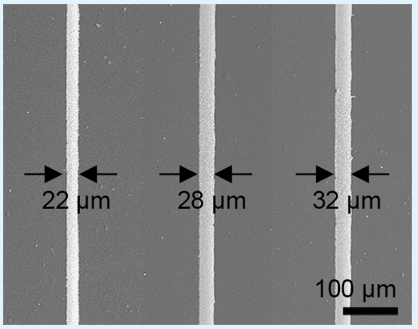


**KEYWORDS:** *screen printing, silver ink, silicon stencils, plastic substrates, printed electronics*

Conventional graphic arts techniques, including screen, gravure, and flexographic printing, have attracted increasing attention for manufacturing of printed electronics on flexible substrates because of their potential for low cost and high-throughput.[1−5] However, their printing resolutions must be improved for high device density and performance. Furthermore, this improvement should be achieved without sacrificing conductivity and printing speed. To meet these goals, innovations are needed not only in the printing process, but also in ink designs.

Screen printing has been widely employed to produce silver electrodes for applications such as transistors, sensors, solar cells, and touch screens.[6−12] This printing method uses a screen mask, typically consisting of a woven mesh, and a patterned stencil attached to the mesh. Ink pressed on the screen mask by a squeegee passes through the portions of the mesh that are not covered by the stencil material. Ink passing through the stencil openings is transferred onto a substrate, leading to a printed pattern. Although this simple technique is potentially cost-effective and fast, the printing resolution is limited to larger than 70 $\mu$m using conventional screen printing meshes with line openings typically no smaller than 40 $\mu$m.[13−16] Although stencils can be produced with fine line openings narrower than 40 $\mu$m, the wire of the mesh tends to block the extremely fine openings and does not allow the ink to pass through the stencil, causing defects.

To improve the resolution of screen-printed silver patterns, researchers have modified screen printing techniques. Erath et al.[16] reported 50 $\mu$m wide screen-printed silver lines by increasing the substrate temperature to reduce the deposited ink quantity and spreading. Schwanke et al.[17] achieved screen printing of 30−40 $\mu$m wide silver lines by modification of the mesh surface to control the adhesion of the ink on the mesh. Even though these approaches have shown promising results, stencils supported by screen masks based on woven mesh have inherent limitations. Recently, a screen printing technique using a single-layer stencil as a screen mask has been developed for graphene patterning.[18] Specifically, a highly defined stencil was fabricated by photolithography from a thin (~90 $\mu$m) silicon wafer with fine line openings as narrow as 5 $\mu$m. This single-layer stencil method without a woven mesh is desirable to produce high-resolution screen-printed silver patterns.

Concentrated silver inks have gained interest for printing conductive traces with high printing resolution and aspect ratio required for high device density and low resistance. Kosmala et al.[19] reported inkjet printing of silver ink with a solid loading up to 45 wt % to achieve thick conductive lines for low resistance. Ahn et al.[20] used highly concentrated (>70 wt %) silver ink for a direct ink writing method for omnidirectional (3D) printing of fine and high aspect ratio silver lines. Concentrated inks have also been used for screen printing. Faddoul et al.[21] studied screen printing with 67−75 wt % silver inks; however, the high

**Received:** March 20, 2015
**Accepted:** June 2, 2015
**Published:** June 2, 2015





DOI: 10.1021/acsami.5b02487
*ACS Appl. Mater. Interfaces* 2015, 7, 12619−12624

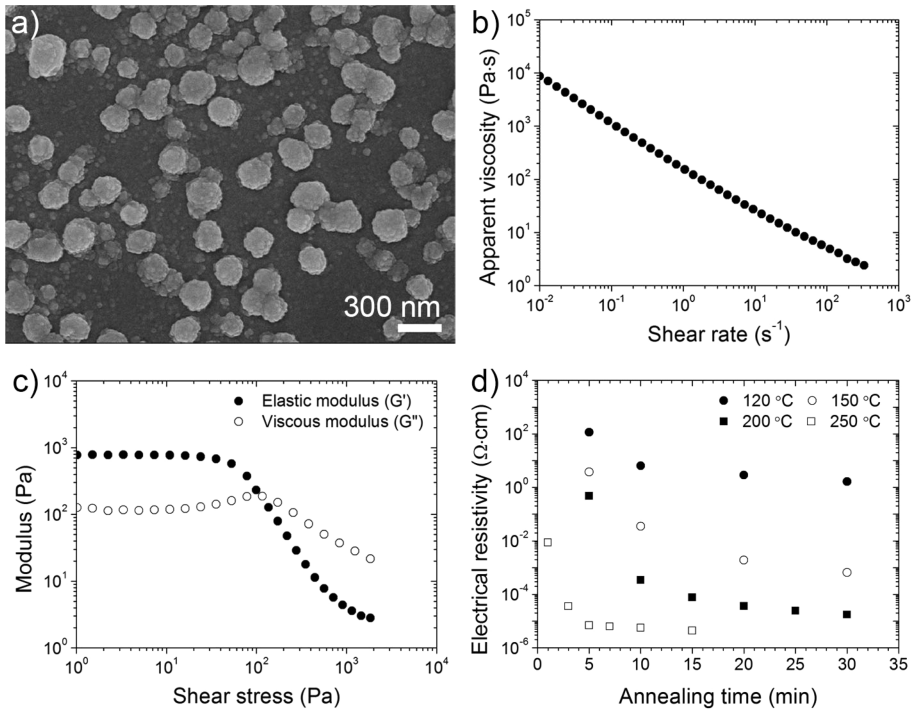


**Figure 1.** (a) Scanning electron microscopy (SEM) image of synthesized silver particles used for the ink preparation. (b) Log–log plot of apparent ink viscosity as a function of shear rate. (c) Log–log plot of shear elastic and viscous moduli as a function of applied shear stress. (d) Semilog plot of electrical resistivity as a function of annealing time for different annealing temperatures.

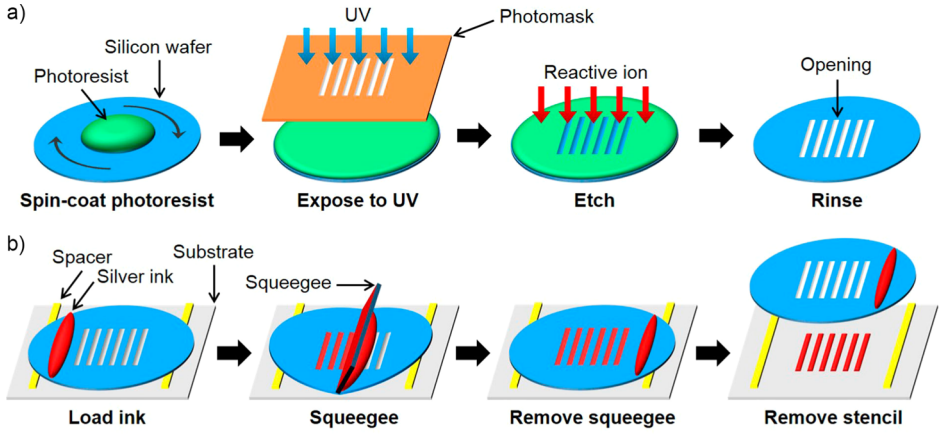


**Figure 2.** (a) Schematic diagrams illustrating the preparation of a silicon stencil using photolithography techniques. (b) Schematic diagrams illustrating of the screen printing method using the silicon stencil and a silver ink.

viscosity of these inks did not allow high-resolution printing with conventional screen masks using a screen mesh.

Here, we demonstrate screen printing of a highly loaded silver ink using the single layer stencil approach for high printing resolution. A highly concentrated silver ink (77 wt %) with sintering temperature below 250 °C is designed for screen printing. Using the high-resolution silicon stencil with line openings ranging from 5 to 50 $\mu$m, we investigate screen printing of the silver ink on flexible substrates and optimize the printing process for creating high-quality silver features. In addition, the printed silver lines are characterized in terms of electrical properties and bendability on flexible substrates.

The highly loaded silver ink used in this study is synthesized with small particle size to facilitate passing of narrow screen openings as well as annealing at low temperature. Silver particles are first synthesized from silver nitrate solution using diethanolamine (DEA) as a reducing agent and poly(acrylic acid) (PAA) as a capping agent (see the Supporting Information for experimental details).[20,22] The size of these particles is determined to be ~5 nm by transmission electron microscopy. Achieving high solids loading at this size scale is difficult because of the high excluded volume associated with each PAA-coated particle.[23] Therefore, a ripening procedure is used to increase the average size to ~200 nm and create a broad size distribution (10–500 nm). Figure 1a shows a scanning electron microscopy (SEM) image of the particles obtained after this procedure; these particles are then concentrated to produce a 77 wt % (24.2 vol %) silver ink in an ethylene glycol/water solution. Ethylene glycol is employed to decrease the drying rate, which improves ink penetration through the stencil and ink transfer. Because PAA is used as capping agent with excess amount (PAA/Ag ≈ 10 wt %) to


DOI: 10.1021/acsami.5b02487
ACS Appl. Mater. Interfaces 2015, 7, 12619–12624

prevent particle agglomeration at high solid loading conditions, the ink is stable over long periods of time when properly sealed. Moreover, if desired, its viscosity could be further tuned by adding additional solvent or changing the mixing ratio of the ethylene glycol/water solution.

The rheological behavior of the silver ink is shown in Figure 1b. The ink is highly viscous, with a viscosity, $\eta$ of $\sim 1 \times 10^4$ Pa s at a shear rate of 0.01 $s^{-1}$. It exhibits a strong shear thinning response, which can be fitted to $\eta = K\dot{\gamma}^{n-1}$ with a power law index ($n$) of 0.2. $K$ and $\gamma$ are the consistency index and the shear rate. The plateau shear modulus ($G'$) is measured to be roughly $1 \times 10^3$ Pa, exceeding the shear loss modulus ($G''$) by nearly an order of magnitude (Figure 1c). From these data, we find that the shear yield stress ($\tau_y$) is approximately 70 Pa. The ink can be transformed into high conductivity features upon annealing at a modest temperature, as shown in Figure 1d. Samples annealed at 200 °C require more than 30 min to achieve $\sim 10^{-5}$ Ω cm. By contrast, upon annealing at 250 °C for short times (≤5 min), the electrical resistivity is found to be $5.0 \times 10^{-6}$ Ω cm, a value approaching that of bulk silver ($1.6 \times 10^{-6}$ Ω cm). The electrical resistivity is lower than that of a similarly prepared highly loaded silver ink in a previous report.[20] This difference can be attributed to the larger particle size (~200 nm vs ~20 nm in the previous work), which leads to reduced contact resistance between particles.

Figure 2a, b illustrates a schematic diagram of the preparation of the silicon stencil by photolithography (see the Supporting Information for experimental details), and screen printing of the silver ink using the stencil. Figure S1 in the Supporting Information depicts the screen printing steps in cross-sectional view. The silicon stencil is separated from a polyimide film (75 μm thick Kapton from Dupont) by 2 mm thick spacers. Use of different spacer thicknesses between 1.5 and 2.5 mm does not change the printing quality significantly. The silver ink is put on top of the stencil and pushed across the stencil openings by a rubber squeegee. This operation is carried out manually at a speed of ~10 cm/s. During the screen printing, the ink passes through the openings and is printed on the substrate. The squeegee and the stencil are then removed from the substrate.

Figure 3a shows the optical microscopy (OM) image of line openings in a silicon stencil (see also Figure S2 in the Supporting Information). The line openings are made with different widths ($w_s$) from 5 to 50 μm. To investigate the effect of the printing direction on screen printing of the silver ink, we carried out printing in two printing directions: perpendicular ($D_\perp$) and parallel ($D_\parallel$) to the line openings. Figure 3b, c compare silver lines printed through the line openings on polyimide substrates for the two different printing directions. With the printing direction $D_\perp$ (Figure 3b), the silver ink is transferred on the substrate through all the line openings from 5 to 50 μm, resulting in high-quality printed silver lines. By contrast, with the printing direction $D_\parallel$ (Figure 3c), line openings wider than 10 μm facilitate good printing whereas those narrower than 7.5 μm do not allow printing at all or yield discontinuous silver lines. The printing procedure was repeated 10 times, with 8 of 10 printings showing the same minimum line openings for good printing, as in Figure 3. The results indicate that the perpendicular printing direction is better for screen printing of fine line openings ($w_s \leq 7.5$ μm) compared to the parallel direction. One explanation is that the squeegee can deform more into the stencil line openings perpendicular to the printing direction, compared to those parallel to the printing direction.[24] As a result, the silver ink underneath the

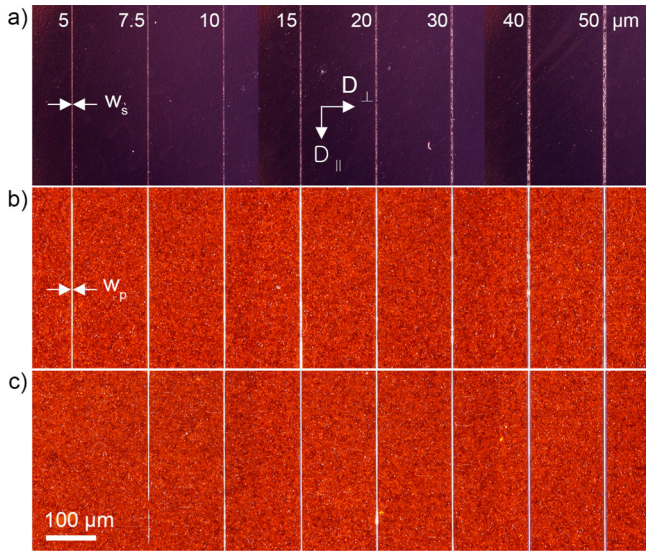


**Figure 3.** (a) Optical microscopy (OM) image of a silicon stencil showing line openings with different widths ($w_s$) from 5 to 50 μm. OM images of silver lines on polyimide films produced by printing with the line openings (b) perpendicular to the printing direction ($D_\perp$) and (c) parallel to the printing direction ($D_\parallel$). $w_p$ is the printed line width.

squeegee in perpendicular openings is pushed more than that in parallel openings, which leads to better contact of the ink to the substrate for the fine lines ($w_s \leq 7.5$ μm).

Figure 4a displays a SEM image of high-quality silver lines printed through line openings with $w_s$ of 5, 7.5, and 10 μm. The printed line widths ($w_p$) were measured using an optical microscope and found to be 22, 28, and 32 μm, respectively. Figures 4b, c, which include data collected from five samples, show the measured $w_p$ and thickness of screen-printed silver lines as a function of $w_s$, revealing that $w_p$ and thickness increase proportionally as $w_s$ increases. The thickness reported is the average thickness from one side to the other side of printed lines using a surface profiler, as shown in Figure 4d. The silver lines prepared from the different printing directions exhibit similar widths and thicknesses for the same line opening, implying that the structural geometry of the printed silver lines is independent of the printing direction. The width of the printed line is larger than that of the opening. Generally, this disparity in screen printing process results from ink spreading after deposition and ink penetration into the gap between the screen and the substrate.[16] In this study, it can be assumed that spreading after deposition is negligible because of the high viscosity and yield stress of the concentrated ink.[20] Therefore, the disparity is mainly due to a continued flow of ink during pushing by the squeegee as the screen and the substrate separate (Figure S3a in the Supporting Information). Even though the stencil and the substrate are in contact during printing, as shown inFigure S1 in the Supporting Information, there is a tiny gap between them. According to the results, ink penetrates into this gap during printing; the amount of penetration is estimated to be 8−11 μm (Figure S3b in the Supporting Information), for $w_s$ from 5 to 50 μm. Nonetheless, the achievement of 22 μm wide silver lines indicates significant resolution improvement for screen printing of conductive silver, compared to previous reports.[13−17] This is even comparable to the printing resolutions of the digital printing techniques including inkjet (typically ≥20 μm) and aerosol jet printing


DOI: 10.1021/acsami.5b02487
ACS Appl. Mater. Interfaces 2015, 7, 12619−12624

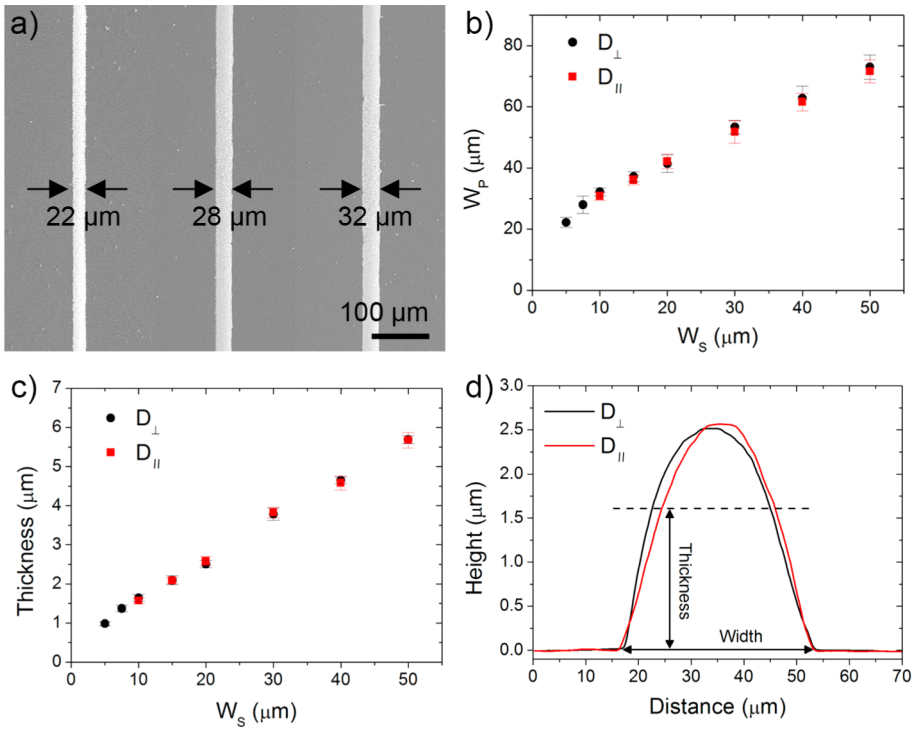


**Figure 4.** (a) SEM image of silver lines screen-printed from 5 (left), 7.5 (middle), and 10 $\mu$m (right) wide line openings. (b) Width ($w_p$) and (c) thickness of silver lines screen-printed with different printing directions of varying $w_s$. (d) Surface profiles of silver lines screen-printed through a same line opening ($w_s$ = 10 $\mu$m) with different printing directions.

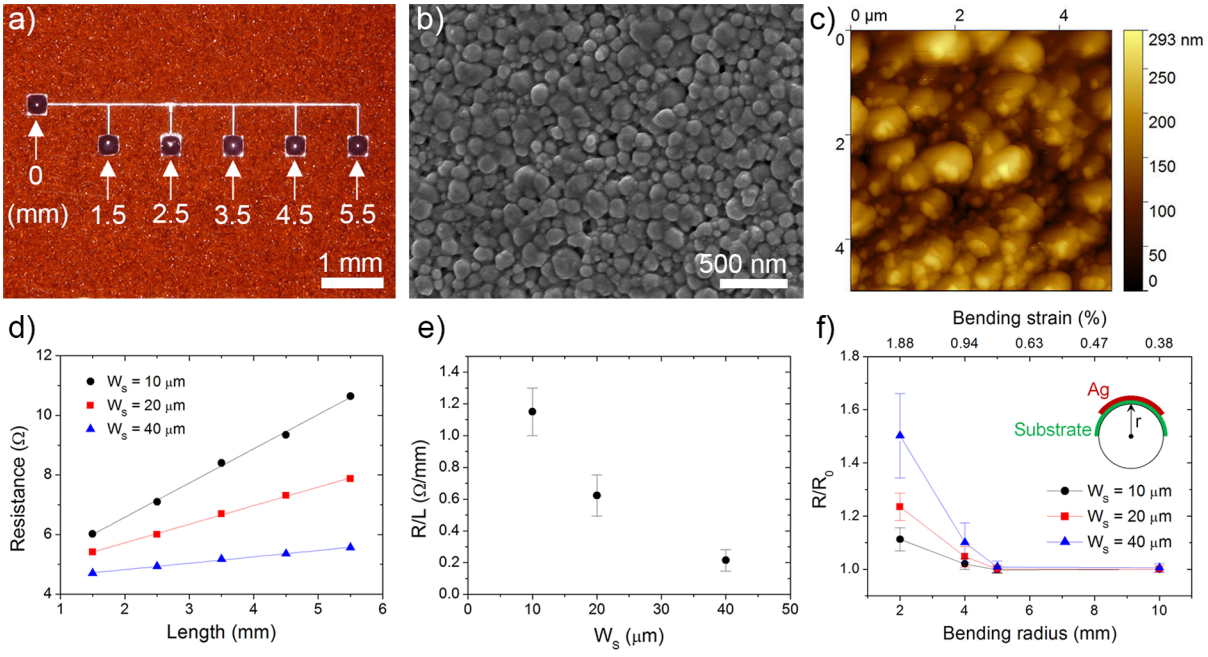


**Figure 5.** (a) OM image of a screen-printed silver pattern for measuring the electrical properties. (b) SEM and (c) AFM images of the silver after annealing at 250 °C for 5 min. (d) Resistance of silver lines measured as a function of length. (e) Resistance per unit length for the screen-printed silver lines with different widths (for $w_s$ = 10, 20, and 40 $\mu$m). (f) Relative resistance of the silver lines after 1000 bending cycles for various bending radii and strains.

(≥25 $\mu$m).[25,26] This improvement can be attributed to the high ink viscosity preventing large ink spreading and the single layer stencil approach enabling ink transfer of the highly loaded ink through extremely fine openings.

Compared to graphene screen-printed using this single layer stencil approach, the screen-printed silver shows higher printing resolution. In a previous report,[18] graphene ink (viscosity: ~13 Pa s at a shear rate of 0.1 $s^{-1}$) was printed through the line openings as fine as 15 $\mu$m, resulting in 40 $\mu$m wide lines. By contrast, the silver ink can be printed through the line openings as narrow as 5 $\mu$m, leading to 22 $\mu$m wide lines. The observation that the silver ink can pass through narrower


DOI: 10.1021/acsami.5b02487
ACS Appl. Mater. Interfaces 2015, 7, 12619−12624

openings than the graphene ink originates from the strong shear thinning behavior of the silver ink, as shown in Figure 1b, because the shear thinning rheology increases the amount of ink deposited on substrates.[27] Moreover, the high viscosity (at low shear rate) and yield stress of the silver ink ($\sim 1 \times 10^3$ Pa s at a shear rate of 0.1 $s^{-1}$) prevent ink spreading after printing as described above, so that the printed line width is widened only by ink penetration into the gap between the screen and the substrate during printing. On the other hand, the low viscosity of the graphene ink (~13 Pa s at a shear rate of 0.1 $s^{-1}$) brings about both of ink penetration during printing and ink spreading after printing. Consequently, widening ($w_p - w_s$) of the silver ink (~20 $\mu$m) is less than that of graphene ink (≥25 $\mu$m).

Nonlinear and complicated silver patterns are also fabricated using the screen printing method. Figure S4 in the Supporting Information displays a stencil opening for a curved line and its corresponding printed silver pattern. Figure 5a shows a printed silver pattern consisting of several lines in different directions. This pattern is used to characterize the electrical properties of the printed silver lines. The pattern has six contact pads to measure the electrical properties for different line lengths of 1.5, 2.5, 3.5, 4.5, and 5.5 mm. Before the measurement, the samples are annealed at 250 °C for 5 min to increase their conductivity, as described above. The SEM image (Figure 5b) shows that the silver particles are sintered during the thermal annealing. The thermal annealing leads to volume shrinkage of the silver, resulting in a decrease of the thickness (Figure S5 in the Supporting Information) by about 12 ± 3%. The root-mean-square (RMS) roughness of the sintered silver over a 25 $\mu$m area is measured to be 48 nm by atomic force microscopy (AFM) measurement, as shown in Figure 5c.

Figure 5d shows the measured resistance of silver lines prepared from line openings with different $w_s$ of 10, 20, and 40 $\mu$m, as a function of their length. The resistance is proportional to the line length, indicating that the silver is uniform along the line. The resistances per length (Figure 5e) are calculated to be 1.15, 0.623, and 0.215 Ω/mm, respectively, for the silver lines printed from the 10, 20, and 40 $\mu$m wide line openings. Based on the structural geometry of the silver lines, the resistivity is calculated to be $5.51 \pm 0.21 \times 10^{-6}$ Ω cm, a similar value to that shown in Figure 1d. Additionally, the flexibility of the printed silver lines (5 mm long) is characterized by carrying out bending tests (Figure S6 in the Supporting Information) for different bending radii ($r$) of 2, 4, 5, and 10 mm, corresponding to tensile strains ($\varepsilon$) of 1.88, 0.94, 0.75, and 0.38%, according to $\varepsilon = d/2r$, where $d$ is the substrate thickness (75 $\mu$m).[28] Figure 5f displays the relative resistance of the conductive lines after 1000 bending cycles. Their resistances are increased for bending radii smaller than 4 mm. The resistance increase of the printed lines using wider openings is higher than that of the lines printed from narrower openings, indicating that the resistance of the thicker lines is increased more than that of the thinner lines. This difference can be attributed to the formation of wider cracks in the thicker silver lines than in the thinner lines during bending tests, as shown in Figure S7 in the Supporting Information. On the other hand, all the printed lines show negligible changes less than 1% for bending radii higher than 5 mm, revealing good bending stability of the printed lines up to 0.75% tensile strain. In addition, printed silver lines annealed at lower temperatures (120 and 150 °C) also exhibit similar results for the bending test, as shown in Figure S8 in the Supporting Information, implying good mechanical bendability up to 0.75% tensile strain regardless of the annealing temperature.

In summary, this study has demonstrated screen printing using highly concentrated (77 wt %) silver inks with shear thinning behavior. The screen printing process using silicon stencils without woven mesh produces fine silver lines with a resolution as high as 22 $\mu$m on polyimide films. The printed silver lines have low electrical resistivity of $5.5 \times 10^{-6}$ Ω cm and good mechanical bendability at tensile strains up to 0.75%. Our approach provides a versatile platform for printing high-resolution, high-conductivity silver lines to generate conductors for flexible electronics.

## ■ ASSOCIATED CONTENT

### Supporting Information

Experimental details; photographs and OM images of silicon stencils and screen-printed patterns; illustration and length of ink penetration; thickness of screen printed lines after annealing; bending test results. The Supporting Information is available free of charge on the ACS Publications website at DOI: 10.1021/acsami.5b02487.

## ■ AUTHOR INFORMATION


### Corresponding Authors

*E-mail: lfrancis@umn.edu.
*E-mail: frisbie@umn.edu.


### Notes

The authors declare no competing financial interest.

## ■ ACKNOWLEDGMENTS

This work was supported by the Multi-University Research Initiative (MURI) program sponsored by the Office of Naval Research (MURI Award N00014-11-1-0690). B.Y.A. was partially supported by the Biorobotics Platform at the Wyss Institute at Harvard University. The authors thank Wieslaw Suszynski and Geoffrey A. Rojas for their contributions to this project. Parts of this work were carried out at the Characterization Facility and the Nanofabrication Center of the University of Minnesota.

## ■ REFERENCES


(1) Perelaer, J.; Smith, P. J.; Mager, D.; Soltman, D.; Volkman, S. K.; Subramanian, V.; Korvink, J. G.; Schubert, U. S. Printed Electronics: The Challenges Involved in Printing Devices, Interconnects, and Contacts Based on Inorganic Materials. *J. Mater. Chem.* **2010**, *20*, 8446−8453.

(2) Li, F. M., Ed.; In *Organic Thin Film Transistor Integration: A Hybrid Approach*; Li, F. M., Ed.; Wiley−VCH: Weinheim, Germany, 2011.

(3) Moonen, P. F.; Yakimets, I.; Huskens, J. Fabrication of Transistors on Flexible Substrates: from Mass-Printing to High-Resolution Alternative Lithography Strategies. *Adv. Mater.* **2012**, *24*, 5526−5541.

(4) *Applications of Organic and Printed Electronics a Technology-Enabled Revolution*; Cantatore, E., Ed.; Springer: New York, 2013.

(5) Kang, B.; Lee, W. H.; Cho, K. Recent Advances in Organic Transistor Printing Processes. *ACS Appl. Mater. Interfaces* **2013**, *5*, 2302−2315.

(6) Bao, Z.; Feng, Y.; Dodabalapur, A.; Raju, V.; Lovinger, A. J. High-Performance Plastic Transistors Fabricated by Printing Techniques. *Chem. Mater.* **1997**, *9*, 1299−1301.

(7) Koncki, R.; Głąb, S.; Dziwulska, J.; Palchetti, I.; Mascini, M. Disposable Strip Potentiometric Electrodes with Solvent-Polymeric




DOI: 10.1021/acsami.5b02487
*ACS Appl. Mater. Interfaces* 2015, 7, 12619−12624

Ion-Selective Membranes Fabricated using Screen-Printing Technology. *Anal. Chim. Acta* **1999**, *385*, 451−459.
(8) Krebs, F. C.; Alstrup, J.; Spanggaard, H.; Larsen, K.; Kold, E. Production of Large-Area Polymer Solar Cells by Industrial Silk Screen Printing, Lifetime Considerations and Lamination with Polyethyleneterephthalate. *Sol. Energy Mater. Sol. Cells* **2004**, *83*, 293−300.
(9) Lim, S. C.; Kim, S. H.; Yang, Y. S.; Lee, M. Y.; Nam, S. Y.; Ko, J. B. Organic Thin-Film Transistor Using High-Resolution Screen-Printed Electrodes. *Jpn. J. Appl. Phys.* **2009**, *48*, 081503−081505.
(10) Bae, S.; Kim, H.; Lee, Y.; Xu, X.; Park, J.; Zheng, Y.; Balakrishnan, J.; Lei, T.; Kim, H. R.; Song, Y. I. Roll-to-Roll Production of 30-Inch Graphene Films for Transparent Electrodes. *Nat. Nanotechnol.* **2010**, *5*, 574−578.
(11) R. Hoenig, R.; Kalio, A.; Sigwarth, J.; Clement, F.; Glatthaar, M.; Wilde, J.; Biro, D. Impact of Screen Printing Silver Paste Components on the Space Charge Region Recombination Losses of Industrial Silicon Solar Cells. *Sol. Energy Mater. Sol. Cells* **2012**, *106*, 7−10.
(12) Vinod, P. N. The Electrical and Microstructural Properties of Electroplated Screen-Printed Ag Metal Contacts in Crystalline Silicon Solar Cells. *RSC Adv.* **2013**, *3*, 14106−14113.
(13) Reese, C.; Roberts, M.; Ling, M.; Bao, Z. Organic Thin Film Transistors. *Mater. Today* **2004**, *7*, 20−27.
(14) Pudas, M. Printing Parameters and Ink Components Affecting Ultra-Fine-Line Gravure-Offset Printing for Electronics Applications. *J. Eur. Ceram. Soc.* **2004**, *24*, 2943−2950.
(15) Brabec, C. J.; Durrant, J. R. Solution-Processed Organic Solar Cells. *MRS Bull.* **2008**, *33*, 670−675.
(16) Erath, D.; Filipović, A.; Retzlaff, M.; Goetz, A. K.; Clement, F.; Biro, D.; Preu, R. Advanced Screen Printing Technique for High Definition Front Side Metallization of Crystalline Silicon Solar Cells. *Sol. Energy Mater. Sol. Cells* **2010**, *94*, 57−61.
(17) Schwanke, D.; Pohlner, J.; Wonisch, A.; Kraft, T.; Geng, J. Enhancement of Fine Line Print Resolution due to Coating of Screen Fabrics. *J. Microelectron. Electron. Packag* **2009**, *6*, 13−19.
(18) Hyun, W. J.; Secor, E. B.; Hersam, M. C.; Frisbie, C. D.; Francis, L. F. High-Resolution Patterning of Graphene by Screen Printing with a Silicon Stencil for Highly Flexible Printed Electronics. *Adv. Mater.* **2015**, *27*, 109−115.
(19) Kosmala, A.; Zhang, Q.; Wright, R.; Kirby, P. Development of High Concentrated Aqueous Silver Nanofluid and Inkjet Printing on Ceramic Substrates. *Mater. Chem. Phys.* **2012**, *132*, 788−795.
(20) Ahn, B. Y.; Duoss, E. B.; Motala, M. J.; Guo, X.; Park, S.; Xiong, Y.; Yoon, J.; Nuzzo, R. G.; Rogers, J. A.; Lewis, J. A. Omnidirectional Printing of Flexible, Stretchable, and Spanning Silver Microelectrodes. *Science* **2009**, *323*, 1590−1593.
(21) Faddoul, R.; Reverdy-Bruas, N.; Blayo, A. Formulation and Screen Printing of Water Based Conductive Flake Silver Pastes onto Green Ceramic Tapes for Electronic Applications. *Mater. Sci. Eng., B* **2012**, *177*, 1053−1066.
(22) Russo, A.; Ahn, B. Y.; Adams, J. J.; Duoss, E. B.; Bernhard, J. T.; Lewis, J. A. Pen-on-Paper Flexible Electronics. *Adv. Mater.* **2011**, *23*, 3426−3430.
(23) Lewis, J. A. Colloidal Processing of Ceramics. *J. Am. Ceram. Soc.* **2000**, *83*, 2341−2359.
(24) Mannan, S.; Ekere, N.; Ismail, I.; Lo, E. Squeegee Deformation Study in the Stencil Printing of Solder Pastes. *IEEE Trans. Compon., Packag., Manuf. Technol., Part A* **1994**, *17*, 470−476.
(25) Lessing, J.; Glavan, A. C.; Walker, S. B.; Keplinger, C.; Lewis, J. A.; Whitesides, G. M. Inkjet Printing of Conductive Inks with High Lateral Resolution on Omniphobic "$R^F$ Paper" for Paper-Based Electronics and MEMS. *Adv. Mater.* **2014**, *26*, 4677−4682.
(26) Mahajan, A.; Frisbie, C. D.; Francis, L. F. Optimization of Aerosol Jet Printing for High-Resolution, High-Aspect Ratio Silver Lines. *ACS Appl. Mater. Interfaces* **2013**, *5*, 4856−4864.
(27) Taroni, M.; Breward, C. J. W.; Howell, P. D.; Oliver, J. M.; Young, R. J. S. The Screen Printing of a Power-Law Fluid. *J. Eng. Math.* **2012**, *73*, 93−119.
(28) Sekitani, T.; Kato, Y.; Iba, S.; Shinaoka, H.; Someya, T.; Sakurai, T.; Takagi, S. Bending Experiment on Pentacene Field-Effect Transistors on Plastic Films. *Appl. Phys. Lett.* **2005**, *86*, 073511.


DOI: 10.1021/acsami.5b02487
*ACS Appl. Mater. Interfaces* 2015, 7, 12619−12624